Contribution from the Department of Chemistry,
Carnegie-Mellon University, Pittsburgh, Pennsylvania 15213

Photochemistry of (μ-Oxo)bis(pentaammineruthenium(III))

DAVID E. BURCHFIELD† and ROBERT M. RICHMAN*

Received May 30, 1984

Irradiation of the title complex in aqueous solution at pH 10 leaves the μ-oxo bridge of the dimer intact and results in substitution of one ammonia by water. The quantum yield is 4×10^{-3} for irradiation wavelengths of less than 500 nm. The photoproduct decomposes to monomeric Ru(III) complexes at a rate of 1.9×10^{-3} s^{-1} at 0 °C; the activation energy for this process is about 10 kcal mol^{-1}. Similar substitutional photochemistry is observed in acetonitrile, but irradiation of the complex in liquid ammonia solution leads to no new products. The nature of the photoactive state is considered.

Introduction

The photochemistry of pentaammineruthenium(III) complexes is generally characterized by simple substitution of a coordinated ligand by water with a low quantum yield and little wavelength variation. Since the lowest excited states in the absorption spectra are charge transfer, but the observed photochemistry is more characteristic of ligand field states, Wells and Endicott[1] suggested that "d–d ↔ CTTM internal conversions are facile among Ru(III) excited states". Indeed, in the case of the analogous Ru(II) complexes, Malouf and Ford[2] have presented strong evidence for initial absorption into a charge-transfer state followed by internal conversion to a substitutionally labile ligand field excited state.

Baumann and Meyer[3] have recently prepared and characterized the cation $[Ru(NH_3)_5]_2O^{4+}$ (D4+), which they considered interesting for its potential to do "extensive, reversible redox chemistry". The photochemistry of this complex interested us, because its M–O–M core is isoelectronic with $(FeTPP)_2O$, for which we have demonstrated a novel photochemical disproportionation.[4] This mechanism of uphill redox chemistry could be useful in solar energy conversion schemes. Hence, we have undertaken a study of the photochemistry of D4+.

Electronic Structure of D4+. The electronic structure of μ-oxo ruthenium dimers was first addressed by Dunitz and Orgel for (μ-oxo)decachlorodiruthenium(IV),[5] $[O(RuCl_5)_2]^{4-}$. This complex is linear in the solid state with net double bonds across the oxo bridge shown in the X-ray crystal structure by the short 1.89-Å Ru–O bond lengths.[6] Overlap of the half-filled t_{2g} orbitals of ruthenium with the oxygen p_x and p_y orbitals generates a π-bonding system extending over the oxo bridge.

For ruthenium(III) μ-oxo dimers two more electrons occupy the π^* orbitals of the bonding scheme (Figure 1). Tatsumi and Hoffmann in their extended Hückel treatment of iron porphyrin μ-oxo dimers have shown that for this case of 10 electrons in the π orbitals the complex is unstable toward bending (Figure 1).[7] The potential energy surface was calculated to be very soft with the bent geometry corresponding to $\theta = 150°$ preferred to the linear geometry by less than 350 cm^{-1} in $[O(Fe(NH_2)_4)_2]^{4-}$. This may be somewhat different for ruthenium dimers due to the larger radial extent of the 4d orbitals and the better energy overlap between $Ru^{III}(t_{2g})$ and $O^{2-}(p_x)$ orbitals relative to Fe^{III} and O^{2-}. However, the same interplay of forces should result in a similarly weak bend stabilization energy.

The one reported crystal structure for a ruthenium(III) μ-oxo dimer, that for $O(Ru(bpy)_2NO_2)_2$, displays this bent geometry with steric interactions limiting the degree of bend to an angle of 157.2°.[8] This complex has a magnetic susceptibility corresponding to 1.8 μ_B per ruthenium ion at room temperature in the solid state.[8,9]

Optical Spectra. The spectrum of D4+ is characterized by two strong, broad absorptions at 500 and 386 nm (Table I).[3] Baumann and Meyer have attributed the 500-nm band to an overlap of $\pi^* \leftarrow d_{xy}$ and $\pi^* \leftarrow \pi^n$ transitions and the 386-nm band to a $\pi^* \leftarrow \pi^b$ transition.

Table I. Optical Spectra of D4+ and D5+

	λ_{max}, nm	ϵ_{max}, L mol^{-1} cm^{-1}	assignment
$[O(Ru(NH_3)_5)_2]^{4+}$ [a]	504	16230	$e_u^* \leftarrow e_g^n$ [b]
	386	5430	$e_u^* \leftarrow e_u$
$[O(Ru(NH_3)_5)_2]^{5+}$ [b]	616	271	$d\sigma^* \leftarrow e_u^*$
	342	25280	$e_u \leftarrow e_g^n$ [b]
	255	2100	

[a] As the PF_6^- salt in acetonitrile. [b] As the Cl^- salt in aqueous solution.

The 500-nm band, if the complex is linear, is an allowed (partly MLCT) transition corresponding to the promotion of a nonbonding electron in an e_g orbital to an antibonding orbital e_u in symmetry. This band is weakly sensitive to solvent dielectric, shifting from 504 nm in acetonitrile to 500 nm in dilute aqueous base (pH 10).

The 386-nm band due to the $\pi^* \leftarrow \pi^b$ transition would be Laporte forbidden in a linear D_{4h} structure. Coupling of the E_u bending vibration or A_{2u} asymmetric stretch to the electronic transition gives this band intensity through a vibronic mechanism.[10]

The electronic spectrum for the singly oxidized dimer $[O(Ru(NH_3)_5)_2]^{5+}$ (D5+) is also listed in Table I for comparison. In this complex the $\pi^* \leftarrow \pi^n$ transition shifts to 342 nm and increases in intensity.[3] A new band appears at 617 nm corresponding to $d\sigma^* \leftarrow \pi^*$ transition. This band is at such a low energy in this $Ru^{3.5+}$ complex dimer because of the already high energy of the π^* orbitals. The energy of the corresponding $d\sigma^* \leftarrow \pi^*$ transition in the III,III dimer is not addressed by Baumann and Meyer in the oribinal report on this complex. Both the $d\sigma^*$ and π^* orbitals are expected to be lower in energy in the 4+ ion so it is not clear where the transition between them will be, but a scan of the near-infrared region reveals no low-energy absorbances for it. The implication then is that the $d\sigma^* \leftarrow \pi^*$ transition for D4+ is at either the same energy or a higher energy than in the oxidized complex and is not observable in the much more intense $\pi^* \leftarrow \pi^b$ and $\pi^* \leftarrow \pi^n$ transitions in the visible region.

Electrochemistry. The reduction of D5+ to D4+ is totally reversible in acetonitrile, acetone, and water (pH 1) with $E_{1/2}$ values of +0.32, +0.25, and −0.175 V vs. SCE in those solvents, respectively.[3] Trace amounts of $[Ru(NH_3)_5OH]^{2+}$ can oxidize $D4^+$, especially at low pH.[11] At pH >9 this instability is checked

† Present address: Department of Chemistry, Bucknell University, Lewisburg, PA 17837.

(1) Wells, W. L.; Endicott, J. F. *J. Phys. Chem.* **1971**, *75*, 3075.
(2) Malouf, G.; Ford, P. C. *J. Am. Chem. Soc.* **1977**, *99*, 7213–7221.
(3) Baumann, J. A.; Meyer, T. J. *Inorg. Chem.* **1980**, *19*, 345–350.
(4) Richman, R. M.; Peterson, M. W. *J. Am. Chem. Soc.* **1982**, *104*, 5795.
(5) Dunitz, J. D.; Orgel, L. E. *J. Chem. Soc.* **1953**, 2594–2596.
(6) Mathieson, A. M.; Mellor, D. P.; Stephenson, N. C. *Acta Crystallogr.* **1952**, *5*, 1985.
(7) Tatsumi, K.; Hoffmann, R. *J. Am. Chem. Soc.* **1981**, *103*, 3328.
(8) Phelps, D. W.; Kahn, E. M.; Hodgson, D. J. *Inorg. Chem.* **1975**, *14*, 2486–2490.
(9) Weaver, T. R.; Meyer, T. J.; Adeyemi, S. A.; Brown, G. M.; Eckberg, R. P.; Hatfield, W. E.; Johnson, E. C.; Murray, R. W.; Untereker, D. *J. Am. Chem. Soc.* **1975**, *97*, 3039–3048.
(10) Drago, R. S. "Physical Methods in Chemistry"; W. B. Saunders Co.: Philadelphia, PA, 1977; p 113.
(11) Kuehn, C. G.; Taube, H. *J. Am. Chem. Soc.* **1976**, *98*, 689–702.

0020-1669/85/1324-0852$01.50/0

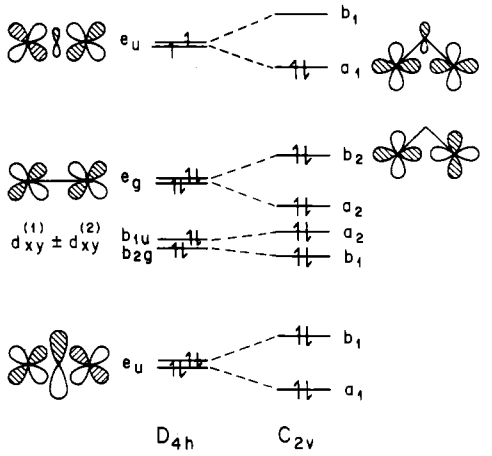

Figure 1. Frontier molecular orbitals originating from the Ru–O–Ru segment of $[(Ru(NH_3)_5)_2O]^{4+}$.

so all photochemistry was performed in dilute sodium hydroxide (10^{-4} M) or 0.10 M triethanolamine, a slightly basic electron-donating redox trap.

Baumann and Meyer have also reported irreversible reduction of D4+ and irreversible oxidation of D5+ in acetonitrile at −1.98 and +1.67 V vs. SCE, respectively.[3] The reduction further lowers the bond order across the oxo bridge; it is therefore not unexpected to find that the D3+ complex is unstable.

Oxidation of D5+ however should lead to a IV,IV dimer. Here, the inability of the ammonia ligands to stabilize the metal centers through π donation as in the polypyridyl and porphyrin[12] dimers probably leads to decomposition of the oxidized species.

Experimental Section

$Ru(NH_3)_5Cl_3$. Chloropentaammineruthenium dichloride was used as supplied by Johnson Matthey Corp. and Alfa Ventron (a distributor for Johnson Matthey), or it was synthesized from $RuCl_3 \cdot nH_2O$ (Alfa) and hydrazine hydrate by the method of Allen and Senoff.[13]

Hydrazine hydrate was prepared by mixing hydrazine hydrochloride with a stoichiometric amount of sodium hydroxide in 95% ethanol. The excess salt was filtered off, the ethanol boiled off, and the hydrazine hydrate distilled at 118 °C.

$[O(Ru(NH_3)_5)_2](PF_6)_4$ (D4+). D4+ was prepared by the perchlorate oxidation of $[Ru(NH_3)_5(OH_2)]^{2+}$ in acetone following the method of Baumann and Meyer.[3] The only change in their procedure was that all reactions from the reduction of $(NH_3)_5RuCl_3$ to isolation of D4+ were done in an oxygen-free drybox under either nitrogen or argon atmospheres. For reactions under nitrogen, argon was bubbled through solutions of Ru(II) to prevent formation of the dinitrogen adduct.

D4+ was precipitated from the reaction mixture either with ether or by adding solid tetrapropylammonium hexafluorophosphate or tetra-*n*-butylammonium hexafluorophosphate. The precipitate was collected by suction filtration, washed with acetone, and analyzed by UV–vis spectroscopy in dilute deaerated aqueous base. Bands at 540 and 342, 295 and 268, and 222 nm indicated contamination by ruthenium red,[14] D5+, and monomeric Ru(III) complexes.

The synthesis was repeated until preparations with no higher oligomers or D5+ were obtained and only moderate amounts of monomeric species were present.

This procedure gave the greatest success, but even this was often not very good. All samples had varying amounts of monomeric Ru(III) species present and anywhere from none to equal amounts of D5+. Higher oligomers were often present and could be detected by a shift in the D4+ band maximum at 500 nm to lower energy and a broadening of that band.

No UV spectrum showed the clean spectral region from 300 to 200 nm represented in Baumann and Meyer's original report on the complex.[3] Photochemistry of D4+ proved very reproducible in the presence of monomeric Ru(III) complexes at long wavelengths ($\lambda_{irr} > 500$ nm) but less so at 386 nm.

No separation technique appeared suitable for purification of D4+ once the synthesis was complete. Column chromatography on either silica or alumina gels using acetonitrile as the eluent resulted in the irreversible binding of D4+ to the support. Cation-exchange chromatography proved highly selective; however, D4+ was oxidized to D5+ in the acidic media (6 M HCl) necessary to elute the complex from the column, and apparently ammonia ligands are labilized in the strong acid. Differential recrystallization tended to concentrate the higher oligomers at the expense of the monomeric species.

Meyer and Taube in kinetic studies on the oxidation of Ru(II) ammine complexes by oxygen discussed the importance of excluding trace amounts of iron.[15] In the synthesis of D4+ it is possible that similar complications arise. In glassware that has not been rinsed thoroughly with distilled water following normal washing, monomeric Ru(III) complexes dominate the products of the dimerization reaction. D4+ is the major product in the rinsed glassware. Since no treatment of D4+ reaction mixtures reliably and repeatedly proved capable of purifying the material, the importance of getting the right complex on the first try merited any extra work cleaning glassware.

Triethanolamine, TEOA. TEOA was obtained as 97% from Aldrich and distilled under vacuum at 100 °C. The first 5% of the distillate contained an impurity that thermally reacted with D4+ in degassed aqueous solution or liquid ammonia to generate the oxidized dimer D5+. This fraction was discarded.

Water. Water was triply distilled: distilled deionized water was distilled under oxygen first from potassium permanganate, then from sodium dichromate, and finally from glass onto a quartz pyrolyzer. Experiments in aqueous solution were first run in this triply distilled water to avoid iron impurities and other materials that might complicate the photochemistry. Photochemistry, however, proved insensitive to the substitution of house-supplied singly distilled water (aluminum pipes) for triply distilled water so all further photochemistry was performed in the house-distilled water.

Acetonitrile. Two grades of acetonitrile were used: reagent grade Eastman 488 and spectroquality Aldrich Gold Label. Photochemistry in both solvents can be traced to impurities but is limiting in the better quality Aldrich solvent, implying no photochemistry for D4+ in absolutely clean acetonitrile (vide infra).

Anhydrous Ammonia. Matheson anhydrous ammonia was used as supplied by condensing the gas into evacuated pressure cells on a vacuum line with dry ice/acetone. The ammonia was frozen in liquid nitrogen and the cell removed from the vacuum line by flame fusing the connecting tube.

Irradiation. For quantum yield determinations a Hanovia 1000-W Hg-Xe lamp was used with a Bausch & Lomb high-intensity monochromator. A water filter was used to absorb infrared radiation before focusing the beam into the monochromator, and low-wavelength cutoff filters were placed in the light path after the monochromator to eliminate higher order harmonics. The monochromator was fitted with diffraction grating 338679 blazed at 300 mm, 1350 rulings/in. Slit combination B with an entrance slit of 2.68 mm and an exit slit of 1.50 mm was used to give a band-pass of 9.6 nm in all experiments. An Oriel low-profile optical bench, Model 1119, was used for the positioning of optical parts.

During irradiations of more than 400 s an area of complete photolysis could be observed in the sample at the focus of the beam. Since the phenomenon resulted in the breakdown of the assumption used in quantum yield determinations, the sample was moved off focus and was agitated at 300-s intervals.

Quantum yield determinations were performed against the Reinicke salt actinometer[16] at 460, 500, 548, and 600 nm and against ferrioxalate[17] at 386 nm.

For preliminary work where higher intensity was desirable, a 300-W tungsten projector bulb (Sylvania ELH) was adapted for use. Corning cutoff filters, Models 2403, 3486, 3385, and 3387, were used to select wavelengths greater than 640, 510, 470, and 450 nm, respectively. The intensity of this source necessitated very short irradiation intervals of 10–30 s, and due to the nature of the photolysis products, this obviated steady-state arguments (vide infra) but proved useful. The intensity was typically 50–100 times higher for this source than for the configuration used for quantum yields.

Flash Photolysis. Flash photolysis spectra were obtained by Dr. M. W. Peterson of Carnegie-Mellon University at the Regional Laser and Biotechnology Laboratories, University of Pennsylvania.[18] Irradiation was effected by the second harmonic of a Nd^{3+}:YAG laser (533 nm) either using it directly or using it to pump a dye laser tuned to 510 nm.

(12) Masuda, H.; Ogoshi, H. *J. Am. Chem. Soc.* **1981**, *103*, 2199.
(13) Allen, A. D.; Senoff, C. V. *Can. J. Chem.* **1967**, *45*, 1337–1341.
(14) Earley, J. E.; Fealey, T. *Inorg. Chem.* **1973**, *12*, 323–327.
(15) Meyer, T. J.; Taube, H. *Inorg. Chem.* **1968**, *11*, 2369–2379.
(16) Wagner, E. E.; Adamson, A. W. *J. Am. Chem. Soc.* **1966**, *88*, 394.
(17) Hatchard, C. G.; Parker, C. A. *Proc. R. Soc. London, Ser. A* **1956**, *A235*, 518.
(18) Rothenberger, G.; Negus, D. K.; Hochstrasser, R. M. *J. Chem. Phys.* **1983**, *79*, 5360.

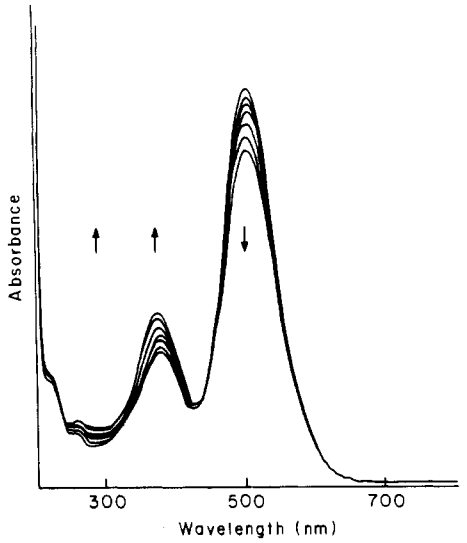

Figure 2. Optical spectra observed upon irradiation of D4+ in aqueous solution with a 300-W projector bulb and a 510-nm cutoff filter.

A xenon flash lamp was used to sample the spectrum from 61 ns to 5.8 μs after irradiation, and a Vidicon tube was used to collect the data.

UV–Visible–Near-IR Spectroscopy. Measurements were made on a Perkin-Elmer 330 spectrometer with a 3600 Data Station. The instrument was fitted with a thermostated cell holder and constant-temperature refrigerated circulating bath (±0.2 °C) for kinetic measurements above −15 °C. For lower temperatures needed when working with liquid-ammonia solutions, a Dewar fitted with optical quartz windows supplied by Professor W. Waddell was suspended in the spectrometer's sample compartment and aligned for minimum scatter.

Electrochemistry. Cyclic voltammetry measurements were performed on a PAR 173 potentiostat/galvanostat and recorded on a Houston Instruments 2000 X-Y recorder. Both the potentiostat and the recorder were driven by a PAR 175 programmer. Voltammograms were referenced to the saturated calomel electrode (SCE). The supporting electrolyte was KPF_6 (Alfa) recrystallized once from hot water and was chosen for its chemical inertness with respect to the ruthenium species studied. All measurements were made under argon.

A platinum-wire electrode was used at potentials between +1.0 and −1.0 V vs. SCE in neutral aqueous solutions; this was cleaned prior to use by the method of Kolthoff and Tanaka.[19,20] At more positive potentials a glassy-carbon electrode was used to retard the oxidation of water, which is catalyzed at a platinum surface.

Continuous irradiation of solutions of D4+ was effected by focusing filtered light from the 300-W lamp on the voltammetry cell and scanning between set potentials at timed intervals to detect unstable intermediates.

Results and Discussion

Photochemistry. $[Ru(NH_3)_5(H_2O)]^{2+}$ absorbs at 420 (sh), 380, and 280 nm with extinction coefficients at 380 and 280 nm of 30 and 624 L mol^{-1} cm^{-1}, respectively.[21] $[Ru(NH_3)_5(OH)]^{2+}$ absorbs fairly strongly at 295 nm (ϵ = 2000 L mol^{-1} cm^{-1}).[22]

Irradiation of a 10^{-3} M solution of D4+ in 1.0×10^{-3} M NaOH results in the spectral changes shown in Figure 2. Under conditions of continuous photolysis a drop in absorbance at 500 nm is observed along with an increase at 365 and 295 nm. Figure 3 shows a plot of the increase in absorbance observed at 295 nm vs. the decrease in absorbance at 500 nm, with the lines corresponding to the different slopes superimposed. The 295-nm band shows a lag time in its development. The 365-nm band grows in at a rate that is dependent on lamp intensity, sample temperature, and irradiation time, implying that it represents an unstable photoproduct.

Under the high-intensity conditions of this experiment, enough of the primary photoproduct (referred to as D4+′) is generated

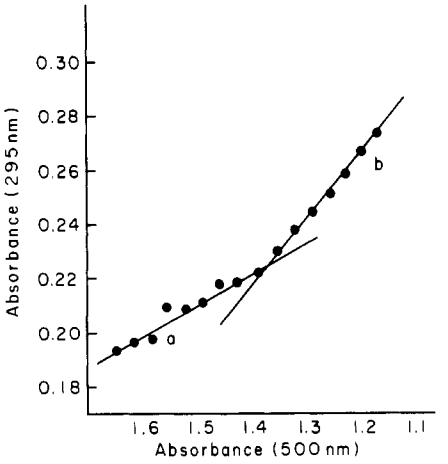

Figure 3. Production of monomeric Ru(III) vs. loss of D4+: (a) slope corresponding to 1:1 production of monomer per D4+ lost; (b) slope corresponding to 2:1 production of monomer per D4+ lost.

to be observed in the visible spectrum. The short irradiation times used at these intensities and the relatively slow decay rate for the intermediate D4+′ invalidate steady-state treatments; each irradiation essentially steps up the concentration of D4+′, and each measurement period allows some of it to react away.

This procedure represented in eq 1 can be described mathematically in terms of a quantum yield for the first step and simple first-order decay kinetics for the second. The concentration of

$$\text{D4+} \xrightarrow{h\nu} \text{D4+}' \xrightarrow{k_1} \text{Ru(III) monomers} \qquad (1)$$

the intermediate [D4+′] at the end of a photolysis period (t_{irr}) is given by the integrated expression in eq 4, where I_0 = intensity of the source (einsteins s^{-1}), ϕ_0 = quantum yield for first step (mol einstein^{-1}) v = volume of the irradiated sample, k_1 = first-order rate constant for D4+′ decay, and t_{irr} = the amount of time the sample was irradiated.

$$\frac{-\mathrm{d[D4+]}}{\mathrm{d}t_{irr}} = \frac{I_0\phi_0}{v} \qquad (2)$$

$$\frac{-\mathrm{d[D4+']}}{\mathrm{d}t_{irr}} = \frac{-I_0\phi_0}{v} + k_1[\text{D4+}'] \qquad (3)$$

$$[\text{D4+}']_{irr,1} = \frac{I_0\phi_0}{vk_1}(1 - e^{-k_1 t_{irr}}) \qquad (4)$$

In the time it takes to remove the sample from the photolysis setup, place it in a spectrometer, and record the spectrum, the intermediate D4+′ continues to decompose at the first-order rate k_1. If this period is referred to collectively as the measurement time t_m, the concentration of D4+′ at the end of this period is given in eq 5.

$$[\text{D4+}']_{m,1} = \frac{I_0\phi_0}{vk_1}(1 - e^{-k_1 t_{irr}})e^{-k_1 t_m} \qquad (5)$$

This quantity is used as the starting concentration for the second integration of eq 3, giving that concentration of D4+′ present after another photolytic cycle $[\text{D4+}']_{irr,2}$. If this procedure is repeated, the expression (6) for the measured concentration of D4+′ de-

$$[\text{D4+}']_{m,n} = \frac{I_0\phi_0}{vk_1}\sum_{i=1}^{n'}(1 - e^{-k_1 t_{irr}})e^{-k_1(t_{irr}+t_m)(i-1)} \qquad (6)$$

velops, where $[\text{D4+}']_{m,n}$ is the measured concentration of the intermediate inthe nth photolytic cycle consisting of an irradiation period t_{irr} and a measurement period t_m.

With the extinction coefficient for the 365-nm band of D4+′ not known and with I_0 of this broad-band source not determined, the concentration formally cannot be calculated. However, the expression in eq 6 can be factored into a constant term and an expression in terms of k_1, t_{irr}, and t_m that will have a different

(19) Kolthoff, I. M.; Tanaka, N. *Anal. Chem.* **1954**, *26*, 632.
(20) Meites, L. "Polarographic Techniques", 2nd ed.; Interscience: New York, 1965; p 435.
(21) Endicott, F. J.; Taube, H. *Inorg. Chem.* **1965**, *4*, 437–445.
(22) Hartman, H.; Bushbeck, C. *Z. Phys. Chem. (Wiesbaden)* **1957**, *11*, 120–135.

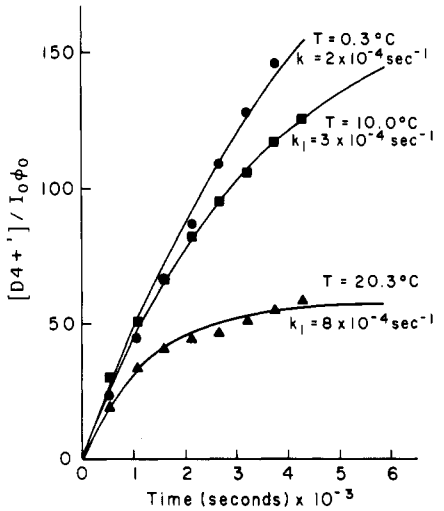

Figure 4. Temperature dependence for the appearance of the 365-nm band in aqueous solution.

curvature vs. n for different combinations of these constants (eq 7).

$$A_{m,n}^{365}(\text{const}) = \frac{1}{k_1}\sum_{i=1}^{n}(1 - e^{-k_1 t_{irr}})e^{-k_1(t_{irr}+t_m)(i-1)} \qquad (7)$$

$$\text{const} = \frac{v}{I_0\phi_0\epsilon_{365}^{D4+}}$$

$A_{m,n}^{365}$ = absorbance at 365 nm after the nth photolytic cycle

Three sets of data were fit to this expression by generating curves corresponding to experimental values of t_{irr} and t_m and different values of k_1. The span of absorbance vs. n data was varied (i.e., the constant was allowed to float) until a good fit of the data to a calculated line was found. The fits for those three sets of data are shown in Figure 4.

In Figure 4 it becomes more apparent that the constant k_1 can determine radically different curvatures in the absorbance vs. n data. For underestimated values of k_1, the early data points tend to miss the curve to the high side; if k_1 is overestimated, the early data points miss to the underside of the calculated curve.

Internal consistency is imposed on the data by optimizing all three fits to the same value of the constant of 5.2×10^2.

The variation of k_1 vs. temperature calculated this way gives an estimate of the activation energy for decomposition of D4+' of 10 ± 4 kcal/mol.

The success of this fit supports the mechanism in eq 1. Since the quantum yield for going D4+ to D4+' is constant throughout the experiment and there is no evidence of D4+ regeneration, no bakc-reaction involving dimerization of the products is included in the mechanism.

Flash Photolysis of D4+. An interesting result is obtained in the flash photolysis of D4+ as to the nature of the intermediate, D4+'. From continuous photolysis there was an expectation that a decrease in absorbance at 500 nm and an increase in absorbance at 365 nm would be observed. The short times between the flash and the probe pulses (≤5.8 μs) would be too fast to observe any buildup of monomeric ruthenium(III) species.

Figure 5 shows the resulting difference spectrum obtained 5.8 μs after irradiating an argon-deoxygenated aqueous solution of D4+ with the second harmonic of a Nd:YAG laser (533 nm). As expected, an increase is observed at 370 nm, but there is little or no bleaching at 500 nm.

This supports the mechanism in eq 1 and provides the additional information that D4+' absorbs at 500 nm with nearly the same extinction coefficient as D4+. The only reason a decrease in absorbance at 500 nm is observed in continuous photolysis is that D4+' is unstable and in the time it takes to scan to 500 nm after photolyzing the sample a significant portion of D4+' has decomposed.

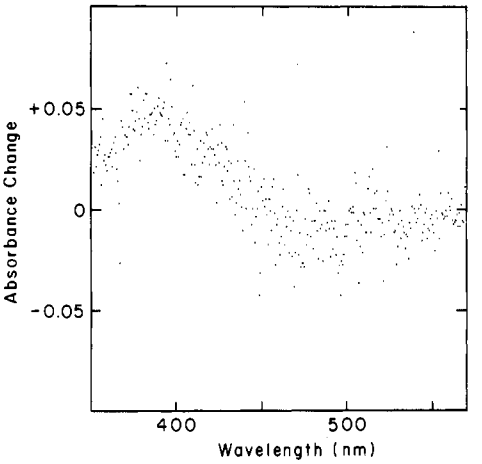

Figure 5. Difference spectrum of 5.8 μm following flash photolysis of D4+ in 0.1 M TEOA at 533 nm.

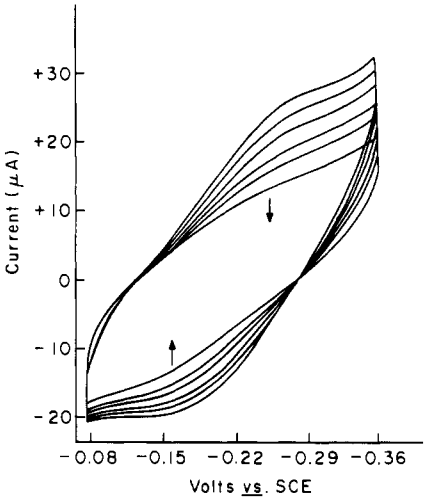

Figure 6. Disappearance of the first photoproduct in aqueous base at 0 °C.

Table II. Comparison of the Visible Spectra and Redox Couples of D4+ and D4+'

	λ_1, nm (ϵ, L mol^{-1} cm^{-1})	λ_2, nm (ϵ, L mol^{-1} cm^{-1})	$E_{1/2}$ (vs. SCE), V
D4+	500 (16 230)	386 (5430)	−0.175
D4+'	500 (<16 000)	365 (~16 000)	−0.21

Electrochemistry. The intermediate D4+' is characterized by a reversible redox couple, with $E_{1/2}$ = −0.21 V vs. SCE, when generated in aqueous base (pH 10) at 0 °C under argon.

Upon cessation of irradiation the results in Figure 6 are obtained. The decrease with time of the peak oxidation and reduction currents is directly proportional to the decrease in concentration of the intermediate; this allows for the calculation of a first-order decay constant k_1 with eq 8,[23] where i_p is the peak current.

$$\log_e (i_{p,t}/i_{p,i}) = k_1 t \qquad (8)$$

The oxidation wave peak currents from Figure 6, plotted against elapsed t, give a first-order rate of decomposition at 0 °C of 1.9×10^{-4} s^{-1}, in excellent agreement for the data obtained at 0 °C spectroscopically at 365 nm (2×10^{-4} s^{-1}).

Nature of the Intermediate. In Table II the visible spectrum and $E_{1/2}$ value for D4+' are compared with those for D4+. It becomes apparent that the two are very similar. The negative

(23) Headridge, J. B. "Electrochemical Techniques for Inorganic Chemists"; Academic Press: New York, 1969; p 44.

reduction potential vs. SCE for the D4+ 5+/4+ couple, the 500-nm $\pi^* \leftarrow \pi^{nb}$ transition, and the 386 $\pi^* \leftarrow \pi^b$ transition are all properties of the π bond in the μ-oxo bridge. That D4+′ substantially shares these characteristics implies that it too is a μ-oxo ruthenium dimer. Whatever changes are occuring, they are peripheral to the bridge itself.

One clue to the nature of the change comes from the increase in extinction coefficient at 365 nm. The higher energy band in D4+ was characterized as a $\pi^* \leftarrow \pi^b$ transition that would be forbidden in a linear structure but that gains intensity by virtue of a small bend in the oxo bridge. Further lowering the symmetry by substitution of an ammonia ligand by water on one side of the dimer should give the transition some dipole character in z, thereby increasing the extinction coefficient.

The allowed $\pi^* \leftarrow \pi^{nb}$ transition would not necessarily gain any intensity as it is already allowed in z.

Support for photosubstitution is found by measuring the pH change in an aqueous sample of D4+ under continuous irradiation following the method of Hintze and Ford for detection of released ammonia.[24] A 3-mL solution of D4+ in argon-deaerated distilled water was irradiated at 500 nm while the pH was measured with a glass electrode. The very low ionic strength necessary to keep D4+ in solution made quantitative pH measurement difficult, but a definite linear rise in pH was recorded over 500 s of irradiation.

If the photochemistry results in the substitution of an ammonia by water, the final photoproducts, the acidoruthenium(III) complexes, should reflect this (eq 10). The observation of 2 equiv

$$[(NH_3)_5Ru\text{–}O\text{–}Ru(NH_3)_5]^{4+} \xrightarrow[2H_2O]{h\nu} [(NH_3)_5Ru\text{–}O\text{–}Ru(NH_3)_4(OH_2)]^{4+} + NH_4^+ + OH^- \quad (9)$$

$$[(NH_3)_5Ru\text{–}O\text{–}Ru(NH_3)_4(OH_2)] \xrightarrow[H_2O]{} [(NH_3)_5Ru(OH)]^{2+} + [(NH_3)_4(OH_2)Ru(OH)]^{2+} \quad (10)$$

of $[(NH_3)_5Ru(OH)]^{2+}$ at 295 nm would seem at first to dispute this mechanism. Rudd and Taube have shown however that the t_{2g}-centered MLCT transition in $[Ru(NH_3)_5py]^{2+}$ at 407 nm is only weakly influenced by replacement of a coordinated ammonia by water.[25] By a similar argument it is plausible that the LMCT transition for both products in eq 10 might occur at the same energy with nearly identical extinction coefficients.

The instability of the intermediate may be due to partial deprotonation of the aquo complex, yielding a μ-oxo hydroxo dimer. In the latter complex, the hydroxo ligand would compete for overlap with the orbitals involved in the μ-oxo bridge, thereby destabilizing it. The subsequent hydrolysis of the oxo bridge would lead to kinetics for decomposition that are first order in concentration of the aquo complex, as is observed (eq 11 and 12).

$$[(NH_3)_5Ru\text{–}O\text{–}Ru(NH_3)_4(OH_2)]^{4+} + OH^- \rightleftharpoons [(NH_3)_5Ru\text{–}O\text{–}Ru(NH_3)_4(OH)]^{3+} + H_2O \quad (11)$$

$$[(NH_3)_5Ru\text{–}O\text{–}Ru(NH_3)_4(OH)]^{3+} + 2H_2O \rightarrow [(NH_3)_5Ru(OH)]^{2+} + [(NH_3)_4(OH_2)Ru(OH)]^{2+} + OH^- \quad (12)$$

Quantum Yield Results. The ultimate photochemistry observed upon irradiation of D4+ is the formation of two monomeric acidoruthenium(III) complexes for each dimer photolyzed. If a period of 10–20 min is allowed to pass following photolysis at room temperature, most of the photogenerated D4+′ decomposes and the absorbance change at 500 nm can be used to compute a quantum yield.

This procedure was followed in generating the data in Table III for the quantum yield variation with excitation wavelength.

Photoredox Chemistry in 0.1 M TEOA. Photolysis of D4+ with a 510-nm cutoff filter in the presence of the electron donor triethanolamine (TEOA) results in the oxidation of TEOA to $TEOA^+$. This is verified following the method of Gratzel and co-workers[26] in basic solution using the reducing nature of $TEOA^+$ upon deprotonation and *N*,*N*-dimethyl-4,4′-bipyridinium(2+) (MV^{2+}) as an electron acceptor.

Table III. Quantum Yield for Photosubstitution of D4+

λ_{irr}, nm	Δt, s	I_0,[a] einstein s^{-1}	$10^{-3}\phi_0$, mol einstein^{-1}
386	780	6.3×10^{-9}	4.5 ± 1
460	420	3.1×10^{-9}	4.3 ± 0.6
500	400	6.8×10^{-9}	4 ± 1
548	360	3.6×10^{-8}	3.2 ± 4
600	800	9.7×10^{-9}	2.9 ± 1

[a] Ferrioxalate actinometer was used at 386 nm,[17] and Reinecke salt at the longer wavelengths.[16]

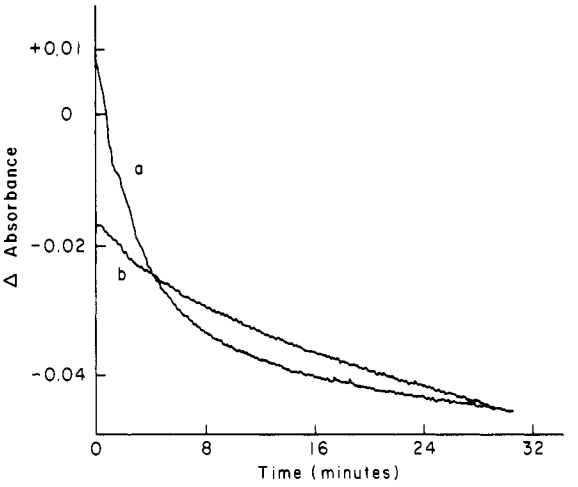

Figure 7. Absorbance at 600 nm following photolysis of D4+ (t_{irr} = 120 s).

$$D4+' + TEOA \rightarrow (D3+') + TEOA^+ \quad (13)$$

$$TEOA^+ \xrightarrow[pH>9]{} TEOA' + H^+ \quad (14)$$

$$TEOA' + MV^{2+} \rightarrow \text{products} + H^+ + MV^+ \quad (15)$$

$$H^+ + MV^+ + [Ru(NH_3)_5(OH)]^{2+} \rightarrow MV^{2+} + [Ru(NH_3)_5(OH_2)]^{2+} \quad (16)$$

Figure 7a shows the initial increase in absorbance at 600 nm due to production of MV^+ and the subsequent drop in absorbance as this is reoxidized by adventitious Ru(III) (eq 16). Overlaid on this, Figure 7b shows the decrease in absorbance at 600 nm in the absence of MV^{2+} and TEOA as the D4+′ produced during irradiation decomposes to monomeric species and Ru(II) catalyzes decomposition of D4+.

In eq 13 D4+′ was used as the oxidant in the initial photoevent. The intermediate D4+′ is implicated by two observations. The first is that in anhydrous ammonia there is no evidence of photochemistry in the presence of TEOA (vide infra). The second is that the loss of D4+ proceeds much in the same manner and with the same rate as it does in the absence of TEOA.

Photochemistry in Liquid Ammonia. D4+ was irradiated in liquid ammonia at high intensities with a 470-nm cutoff filter. Under these conditions, there should be no observable photosubstitution, since the product is starting material, which is stable in liquid ammonia. These are ideal conditions for observing a low

(24) Hintze, R. E.; Ford, P. C. *J. Am. Chem. Soc.* **1975**, *97*, 2664.
(25) De Rudd, F. P.; Taube, H. *Inorg. Chem.* **1971**, *10*, 1543. See also: Ford, P. C.; Kuempel, J. R.; Taube, H. *Inorg. Chem.* **1968**, *7*, 1976.
(26) Kalyansundaram, K.; Kisi, J.; Gratzel, M. *Helv. Chim. Acta* **1978**, *61*, 2720.

quantum yield photodisproportionation, which should yield a ruthenyl ion and hexaammineruthenium(II) (eq 17). However, there is not observable photochemistry, indicating that the upper limit for the photodisproportionation quantum yield is about 2 × 10^{-6}.

$$[(NH_3)_5Ru—O—Ru(NH_3)_5]^{4+} \xrightarrow[NH_3]{h\nu} [(NH_3)_5Ru{=}O]^{2+} + [(NH_3)_6Ru]^{2+} \quad (17)$$

When TEOA is added to an anhydrous ammonia solution of D4+, there is also no observed photochemistry. This is peculiar since the TEOA should be able to weakly bind to a coordinatively unsaturated dimer generated in photolysis. In this case it could be that the strong affinity that ammonia has for Ru(III) and the lability of oxygen donors on Ru(III) combine to make the back-reaction fast enough that no photochemistry is observed.

Photochemistry in Acetonitrile. Irradiation of the 500-nm band of D4+ in reagent grade acetonitrile results in a large increase in absorbance at 382 nm with virtually no change in absorbance at 500 nm. In light of the photosubstitution occurring in aqueous solution and the knowledge that the aquo nonaammine intermediate D4+′ has nearly the same absorption envelope at 500 nm, it is apparent that what is occurring here is similar. This result in fact supports the interpretation of the aqueous photochemistry, for in acetonitrile the photoproduct is thermally stable at room temperature.

If one assumes a simple model of species A and B with B absorbing at the irradiation wavelength, then the quantum yield expression including internal filtering is

$$A \xrightarrow{h\nu} B \quad (18)$$

$$-\frac{dC_A}{dt} = \frac{I_0\phi_0}{v}(1 - 10^{-\sum \epsilon_i c_i}) \frac{\epsilon_A C_A}{\epsilon_A C_A + \epsilon_B C_B} \quad (19)$$

Since $\epsilon_B^{530nm} = \epsilon_A^{530nm}$, the exponent and the denominator on the right side of the eq 19 are constant. Substituting $[A]_0 - [B]_t$ for $[A]_t$ yields the expression

$$-\log_e ([A]_0 - [B]) = \frac{I_0\phi_0}{v}(1 - 10^{-\epsilon_A[A]_0})\frac{t}{[A]_0} - \log_e [A]_0 \quad (20)$$

Thus, a plot of $-\log_e ([A]_0 - [B])$ vs. irradiation time t should be linear. Shown in Figure 8 is such a plot where the left side of eq 20 was evaluated by assuming an extinction for B of 82 000 L mol^{-1} cm^{-1} at 382 nm. This extinction coefficient was determined by minimizing the curvature in the data points, but it generated the consistent conclusion that ϕ_0 must be near 4 × 10^{-3} mol $einstein^{-1}$.

Whatever the nature of the substitution product, the quantum yield for its formation is very similar to that measured for aqueous photosubstitution. This argues strongly for a dissociative mechanism consistent with what has already been observed in thermal and photochemical substitution on Ru(II).

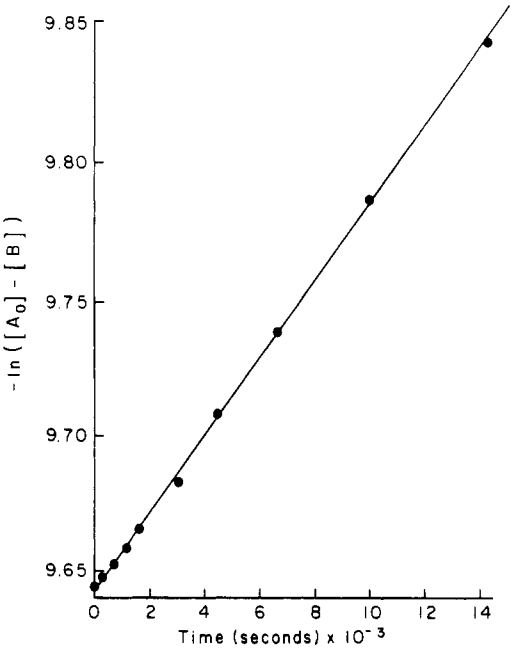

Figure 8. Appearance of the first photoproduct in reagent acetonitrile as a function of irradiation time (λ_{irr} = 530 nm).

This result was not reproducible when spectroquality acetonitrile was substituted for reagent grade, indicating that an impurity was responsible for trapping D4+*. Although it was not possible to identify this impurity or the photoproduct, these results are nonetheless of value in support of the data in aqueous solution.

Nature of the Excited State. What is observed in the decaammine is photosubstitution, and this occurs with a relatively constant quantum yield vs. energy profile. From these results and the similar results in acetonitrile, it is clear that population of the $\pi^* \leftarrow \pi^{nb}$ state induces substitution. However, it is more reasonable for such a result to obtain from a ligand field state, so the following mechanism of internal conversion is suggested.

The high energy of the half-filled π^* orbitals of the μ-oxo bridge makes the population of a $d\sigma^*$ orbital possible. It has already been noted that the $d\sigma^* \leftarrow \pi^*$ transition occurs at 617 nm in D5+ (Table I), so it may be near 500 nm in D4+. If so, the $d\sigma^* \leftarrow \pi^*$ state could be responsible for the observed photosubstitution.

Acknowledgment. We thank Dr. M. Peterson for helpful comments and for performing the flash photolysis experiments. We thank D. Herrup for experimental assistance. This research was supported by the Office of Basic Energy Sciences of the Department of Energy.

Registry No. TEOA, 102-71-6; D4+, 72049-57-1; NH_3, 7664-41-7; H_3CCN, 75-05-8; $[(NH_3)_5Ru(OH)]^{2+}$, 38331-41-8; $[O(Ru(NH_3)_5)_2]^{5+}$, 72049-56-0.